

# Responsive Kirigami: Context-Actuated Hinges in Folded Sheet Systems

Jingyang Liu<sup>1,2</sup>, Jasmine (Chia-Chia) Liu<sup>2,3</sup>, Madeleine Eggers<sup>1,2</sup> and Jenny E. Sabin<sup>1,2</sup>

<sup>1</sup>Architecture  
Cornell University  
Ithaca, USA  
jl3449@cornell.edu

<sup>2</sup>Sabin Design Lab  
Cornell University  
Ithaca, USA  
jsabin@cornell.edu

<sup>3</sup>Material Science  
Cornell University  
Ithaca, USA  
cl777@cornell.edu

## ABSTRACT

This paper explores the possibilities of active kirigami geometry — folding with the addition of strategically placed cuts and holes — through geometry, simulations, and responsive materials exploration. We have developed a novel method for kirigami pattern design through mesh optimization of surfaces, distribution of tucks across the discretized mesh, and the addition of cut and fold patterns. Based on our previous materials research on dual composite kirigami materials in 2016, we propose to focus on both one-way and two-way actuated materials, including shrinky dink films, shape memory alloys, and shape memory polymers. We have successfully characterized the materials, and as a proof of concept, produced models that utilize the above-mentioned materials as environmentally-actuated hinges in folded sheet systems (2D to 3D).

## Author Keywords

adaptive architecture; kirigami; simulation and modeling; computational geometry design; material design; programmable matter; hinge design; actuation, matter design computation

## 1 INTRODUCTION

As part of two projects funded by the National Science Foundation in the Sabin Design Lab at Cornell University titled, eSkin and Kirigami in Architecture, Technology, and Science (KATS), this paper is one product of ongoing trans-disciplinary research spanning across the fields of architecture, bio-engineering, materials science, physics, electrical and systems engineering, and computer science. Like origami (ori = folding, gami = paper), the origins of kirigami comes from the art of folding paper, but with the addition of cuts and holes. The word comes from the Japanese kiru, “to cut,” a geometric method and process that brings new techniques, algorithms, and processes for the assembly of open, deployable, and adaptive structural elements and architectural surface assemblies. We ask, how might architecture respond ecologically and sustainably whereby buildings behave more like organisms in their built environments [1]. This interest probes flexible geometric systems such as kirigami for design models that give rise to

new ways of thinking about issues of adaptation, change, and performance in architecture. Broadly speaking, these models and prototypes engage geometric and biomimetic principles in the synthesis and design of new materials that are adaptive to external inputs, such as heat, light, and human interaction [2]. With kirigami, we strive to communicate three-dimensional (3D) geometry, structures, and features using two-dimensional (2D) representations and sheet systems that follow the concept of "Interact Locally, Fold Globally," necessary for deployable and scalable architectures. In previous projects, we have produced a room-scale prototype for an adaptive architecture system, which uses a combination of novel surface materials and nitinol linear actuators to react and respond to its environment and inhabitants [3]. Together, this synthesis of design, material, and kirigami-programming allows a small set of simple actions to manifest complex emergent behaviors. In recent work, we have moved away from cumbersome mechanical systems and energy-heavy complex mechatronics and towards integrated panel-and-hinge assemblies that feature 3D printed programmable geometry and materials capable of controlled, elastic response to stimuli [4]. In this paper, we document our latest work on kirigami-steered assemblies for adaptive composite systems that are programmable in both one-way and two-way actuated materials, including shrinky dink films, shape memory alloys, and shape memory polymers. The assemblies with thermal sensitive materials enable context-based actuation in that the actuated hinge is passively actuated by the thermal environment.

## 2 MATERIALS AND METHODS

### 2.1 Geometric Approach of Kirigami Pattern Design

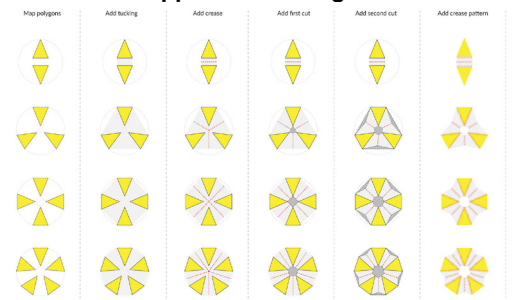


Figure 1. Unfolding a hexagonal pyramid into two-dimensional kirigami pattern

The objective of this section is to transform a given three-dimensional freeform surface into a two-dimensional kirigami pattern and validate the process by reshaping the 2D plane into 3D surface by both simulation and physical test. The approach presented in this section consists of two parts. The first part describes a framework for kirigami pattern design at the local level where multiple pyramid shapes are used to demonstrate the process of unfolding and folding. Built upon this local-level research, a generative computational method for designing 2D kirigami patterning for 3D global freeform surfaces is introduced. The given surface is initially approximated by triangular mesh, which is then decomposed into polygons and isometrically mapped onto a 2D plane. The approach utilizes folds and creases to connect overlapped edges of polygons. Cuts are applied to solve vertex-intersection and edge-intersection in the folding process.

*Designing a Kirigami Component: Part to Whole*

Several analytical studies have been done in computational kirigami and origami that aim to generate and simulate the folding of a 2D pattern into a 3D surface. For example, David Huffman proposed an origami tessellation method for both straight and curved folding using the Gauss map [5]. In comparison, the tree method generates a tree line graph on a squared sheet of paper to fold the planar pattern into a desired 3D shape [6]. In Tachi's study [7], a method is presented for generating a fold pattern based on an arbitrary three-dimensional mesh, which serves as the goal shape and primary input. Collaborator, Fabrizio Scarpa and Randall Kamien [8], developed a rule set to create 3D structures from a flat sheet using bending, folding, cutting, and pasting. Our design approach augments and builds upon Tachi's and Kamien's research to combine folding and cutting for the generation of a 3D goal shape from 2D flat paper. At the local level, we started by unfolding a polyhedral shape. The faces of the given polyhedral shape were initially decomposed into individual polygons and isometrically mapped onto a 2D plane. The gap between polygons is a quadrilateral symmetric trapezoid (see Figure 1). The crease pattern is generated within the gap between adjacent polygons where the gap is constrained to be symmetric. The valley crease is defined by connecting the midpoint of a non-equal edge of a given quadrilateral trapezoid. The width of the crease pattern may be modified to changes in the curvature of the valley fold. The stiffness of the folding crease is programmable by modifying the porosity and configuration of the crease pattern, as shown in Figure 1. For polygons sharing a vertex, the surrounding vertices are folded into one shared vertex. The initial cut covering area is defined by the shared vertices of

connected faces. To avoid intersections of the tucked folds, secondary cuts are applied. The area of the secondary cut is defined by the angle between adjacent mesh faces and the width of the hinge (see Figure 1).

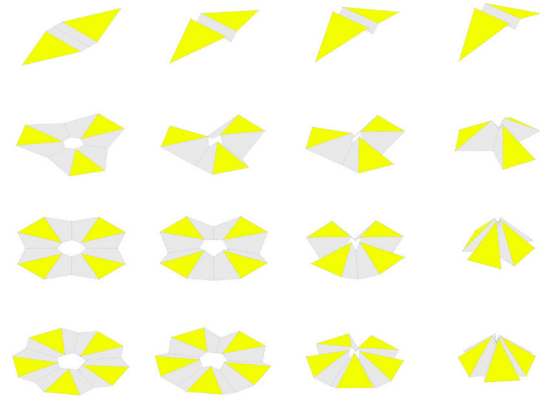


**Figure 2.** Simulation of reshaping two-dimensional kirigami pattern into three-dimensional pyramid

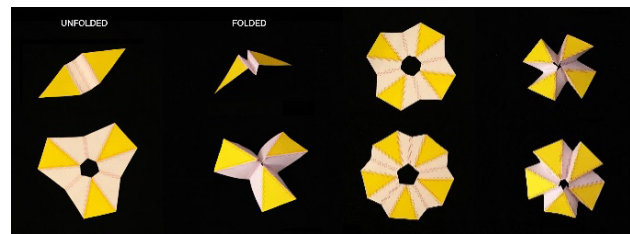


**Figure 3.** Physical model of the unfolded and folded states, demonstrating the validity of simulations

The geometric approach described was implemented and simulated in Rhinoceros 3D, a commercial 3D computer graphics and computer-aided design application software and Grasshopper 3D, a graphical algorithm editor integrated in Rhinoceros 3D. To justify the geometric approach, we are interested in the role of kirigami patterning on the global form of the folded sheet as a generative design strategy over optimization of the stress distribution upon each face. As a result, we did not elect to use finite element modeling to analyze stress distribution as a starting point. Building upon research work introduced by Schenk [9], we translated the 2D kirigami pattern mesh model into a pin-jointed truss framework. The vertex of each mesh face was represented as a pin-joint, and every fold line by a bar element. With input information of the folding angle between each mesh face, the displacements of vertex coordinates can be calculated using coordinate transformation,  $d_i = Td$ , where  $T$  is the transformation matrix and  $d$  is the nodal displacement,  $\theta$  is the change in angle. The kirigami pattern mesh was dynamically reconstructed based on translated mesh vertices

to simulate the folding process. The simulation of 2D kirigami pattern folding is demonstrated in Figure 2. To verify the simulation, we folded paper models into the desired goal shapes (see Figure 3).

#### Kirigami Tessellation Based on Freeform Surface

The proposed kirigami component design is primarily based on the input mesh. As we used Rhinoceros 3D to design this complex geometry, translation from surface into discrete meshes is required for the initial setup. The discrete meshes can then be unfolded onto the 2D kirigami pattern through mapping and adding tucks and cuts as we introduced previously. As a first step, the interactive design pipeline for generating the kirigami pattern uses the Enneper surface as input (see Figure 4).

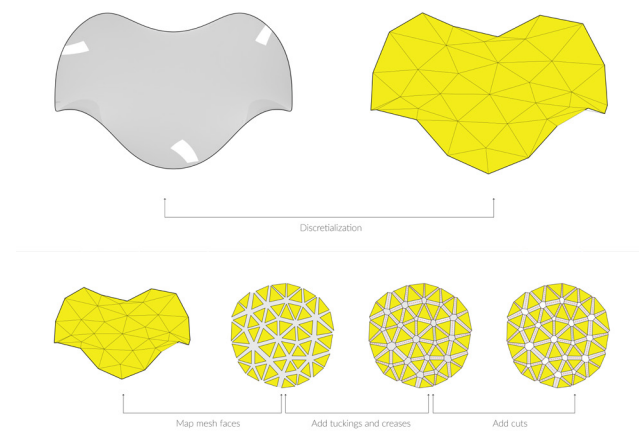


**Figure 4.** Pipeline of unfolding a given three-dimensional Enneper surface onto two-dimensional kirigami pattern

Many commercial computer-aided design (CAD) tools including Rhinoceros 3D have functions for translation between mesh and surface. However, we found that the mesh faces generated by these default functions were uniform and regular. The approximation of a given global freeform surface using uniform mesh faces causes high deformation when the mesh resolution is set at a low level. However, if we increase the mesh resolution to obtain a high approximation rate of the input surface, the number of mesh faces will increase causing complexity for folding. Inspired by the adaptive remesh method proposed by Peraire [9], we proposed an alternate mean-curvature-based mesh representation algorithm. The algorithm consists of three steps. Initially, the mean curvature of the input surface was analyzed and stored as topological information. Secondly, an anisotropic mesh subdivision based on surface mean curvature was introduced. Additional iterations of subdivision were processed in areas where the surface area curvature was higher to ensure that enough triangles were

populated to maintain curvature. Next, each edge of the mesh faces was set as a spring with certain stiffness and targeted length. The value of the targeted length was determined based on the mean curvature at the start and end points of each edge. Using the particle system, Kangaroo Physics developed by Daniel Piker for Grasshopper 3D [10], the mesh was relaxed to achieve equilibrium.

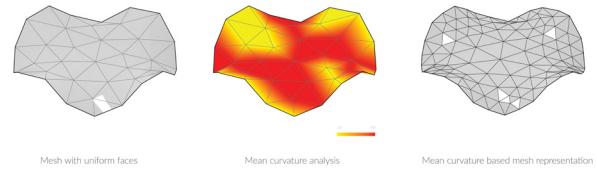


**Figure 5.** Mesh representation based on mean curvature

To validate the unfolding algorithm, we used the simulation method we proposed in section 2.1.1 to simulate the folding process from 2D kirigami pattern into 3D Enneper surface (see Figure 6). A paper model was fabricated and folded to validate the simulation (see Figure 7).

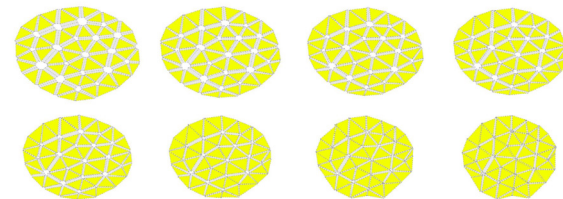


**Figure 6.** Simulation of reshaping two-dimensional kirigami pattern into three-dimensional Enneper surface

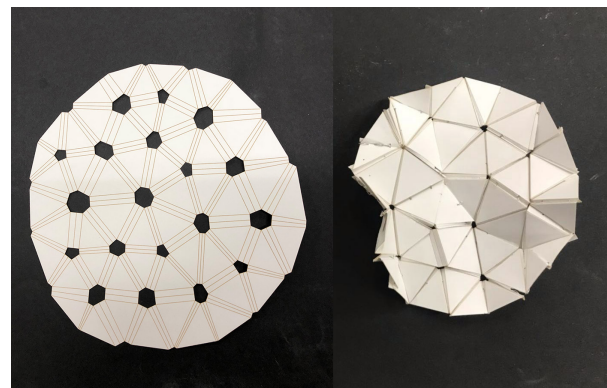


**Figure 7.** Paper model of folded Enneper surface

## 2.2 Material Characterization

Our final phase of material explorations builds upon our previous investigations with silicone and 3D printed ABS auxetic composites from our work in 2016, which utilizes a two-material system to induce various types of actuation [4]. Rather than focus on the two-dimensional auxetic composite body, our investigations push forward active elastic folding with global elastic deformation, and towards

environmentally-actuated hinges in folded sheet systems (2D to 3D).

The material systems conceptually relate to the 2016 composite system through a layered, unit-based system. The actuating material is the ‘skeletal system’ and a flexible, inactive material forms the body that distributes the actuation forces across the larger matrix of units. Our investigation of actuating materials focused on three types of materials: ‘Shrinky Dink’ film (SDF), shape-memory alloy (SMA), and shape-memory polymer (SMP). The selection of materials is based on commercial availability and cost.

Pre-strained polystyrene — known colloquially as the children’s toy “Shrinky Dinks” — is a commercially available, optically transparent plastic sheet material that undergoes planar shrinkage when heated. The recoiling of the microscopic polymer chains in the polystyrene sheets exhibit 1-way shape change and are irreversible in nature. Once shrunked, it cannot relax and go back to its original state.

On the other hand, shape-memory alloys can undergo two-way shape change. Shape-memory alloys are alloys that ‘remember’ their original shapes and can be restored to their original shape if exposed to heat or light while deformed. The resting shape of a SMA is determined manually. When heated to above the transition temperature, the shape of the wire at the phase-change temperature is processed into the impart memory of the initially shaped state. Once the shape has been set and cooled down to room temperature, the wire can be further deformed, and then restored to the set shape by applying heat to a threshold temperature. Our SMA investigation augments the Sabin Design Lab’s 2014 project, *Colorfolds*, which made heavy use of nitinol springs, a type of commercially available pre-formed SMA spring that relaxes in the presence of heat and contracts when the heat source is taken away. Instead of the spring configurations in *Colorfolds*, we investigate nitinol wires, which require less energy input in actuation.

The third material that we investigated to innovate hinge design in kirigami actuated matrices, is shape-memory polymers. SMPs are an emerging type of dynamic (‘actively moving’) polymers with shape-retention capability and thermally-induced transformation properties. SMPs are formed into their resting shape through conventional plastic molding or extruding processes and can afterwards be deformed and ‘set’ into its deformed shape. The resting shape can be reset when quenched after heating above the transition temperature between plastic state and elastomeric state [11]. When exposed to a certain stimulus — most commonly heat or light — SMPs revert back to their initial states. Though less widely available than SDF and SMAs, SMPs have several advantages over their counterparts: for SMPs, the cycle of programming, deformation, and recovery takes place in a much shorter timeframe than that of metallic shape-memory alloys, as well as allowing a much greater range of motion between the initial and deformed states.

Also, SMPs generally require less energy input than SMAs, as the threshold temperature of the polymers is lower than that of metal alloys. In addition, SMPs are far more robust than shrinky dink film and are able to withstand much higher forces without tearing.

In order to obtain the final programmable property, we need to characterize the materials described above. The listed materials, shrinky dink film and SMAs, have the potential of being utilized in hinge designs to actuate system responses. In the process of actuation, the forces that the materials generate are the most important variable.

A testing frame is set up as shown in Figure 8. A Vernier Force Sensor is fixed to the top of the stand; the test samples are attached to the sensor and the bottom of the stand. A 1300W heat gun is then used to provide energy input to various samples. For the shrinky dink film, force is a complex variable that is a combination of the function of energy-input, time, and total sample surface area. We have determined five different widths: 0.25”, 0.5”, 0.75”, 1”, and 1.25”. There are 10 strips of shrink dink film for each width, and all samples are 3” in length. As the test samples receive heat, reach threshold temperature, and retract to their original shape, the sensor is able to document the force change over time.

Because the nitinol wires and the SMPs are manufactured to a certain fixed wire radius, the sample width is not a considered variable in the force control experiment. Nitinol wires are cut into 20 pieces of 3” samples. All the samples are heated above the phase-transition temperature and folded in half. After quenching with cold water, the wires are re-configured back to a straight geometry, and attached to the force stand and sensor. Then, the heat gun is used to heat the wires to the threshold temperature (40 degrees Celsius) and the force required to revert the wires back to the original shape is extracted from the Vernier sensor and post processed.

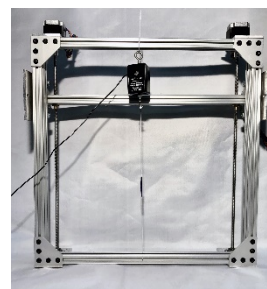


Figure 8. Testing frame setup for characterization

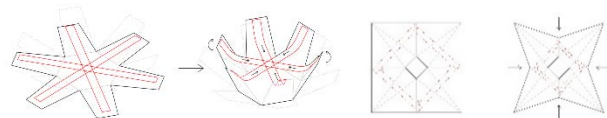


Figure 9. Shrinking material (red) acting as a folding agent on a kirigami body. Upper: SDF acting on a square pyramidal unit. Lower: SDF acting on a cross-body folding unit.

The characterizations of SMPs are similar to those of SMAs. The polymer strips have a fixed width of [ ] and are cut into pieces of 3"-long samples. Because the actuated force generated by one piece of the SMP is too small to be documented without significant errors, we have glued 3 pieces of SMPs together, and further characterize as one sample in the experiments. The SMP samples are heated above the transition temperature, folded in half, quenched in cold water, and re-configured back to a straight geometry. 15 samples were then analyzed with the same techniques as those of nitinol wire characterization.

### 2.3 Hinge Actuation Design

These three active materials each have the potential to be combined or utilized in composite active material systems. Hinge design was explored through a forward process, testing material actuation on one single unit to allow us to better understand material interactions and the potential for local programmability at the unit scale. Data and knowledge gained at the single unit design scale informs larger arrays of tessellated units and actuation for inverse-process geometry.

Hinge actuation using SDF was first explored on a single-hinge scale, then on a unit scale involving several hinges. Our component-based investigation began with testing the SDF using a forward process of investigation, examining the effects of different SDF placement and crease arrangements at the unit scale.

The units generated to test the SDF actuation system were made of scored bristol paper, with individual .5" wide SDF strips affixed at both endpoints to the paper body by rudimentary metal staples, a solution chosen for its ability to withstand heat while firmly attaching the SDF strip with the smallest possible point of restraint, as well as being readily available and cost-effective. Two unit types were made, each with a different SDF-body relationship.

The polygonal unit was a square with a square hole at the center, rotated 45 degrees. Four triangular facets are formed by scoring lines connecting the corners of the outer square to the nearest two corners of the inner square hole. By placing another scored line orthogonally connecting the corner of the inner square hole to the midpoint of the nearest side of the outer square, valley folds are created (see Figure 9). The SDF is attached on the right side of the valley fold as close as possible to the crease, connected to the same point relative to the crease on the adjacent side. When the SDF shrinks while pinned in place on the two ends, the crease makes a valley fold which pulls the global geometry together (see Figure 11).

The cross-body fold unit was composed of 6 free-end flaps connected to a single body, with the SDF attached to the endpoints of opposing arms (see Figure 10). When heat is applied, the SDF shrinks toward the center and pulls the opposing arms inward and together, contracting the unit as a whole. One advantage to this test unit was that it was easy to heat uniformly. Aiming the heat gun at the intersection point

of the radially-arranged SDF strips actuated all of them more or less at the same time, allowing for smooth and immediate folding. This unit type also allowed us to quickly examine the actuation properties of the SDF on a unit of related hinges without the need to deal with the greater forces associated with actuating hinges connected in series that would be dependent on each other to actuate.

### 3 RESULTS

Our SDF test units served as intermediary steps to develop methods for inverse-process sheet folding to test unit types and their corresponding geometric logic. The two forward-process test units were made for the purpose of developing an actuation system for the polyhedral shapes shown in Figure 1 and for smaller prototypes following the same logic as the global geometries in Figures 4-7. To test the units, the units were held in place while a standard 1500W heat gun was used to manually apply heat. The SDF material we used has a transition temperature of 165 degrees Celsius, and we found that reaching the transition temperature took between 4 and 8 seconds of constant heat application. (see Figure 17). The cross-body units tended to actuate unevenly, with one end of the SDF strip reaching the transition phase before the other. The units would often have three adjacent arms pull inward before the connected opposing arms would be brought together. This effect foreshadowed a larger problem that appeared as we further developed methods for actuating hinges connected in series. This would need to happen in the generation of a multi-unit agglomeration system or inverse-process geometry with non-uniform actuation.

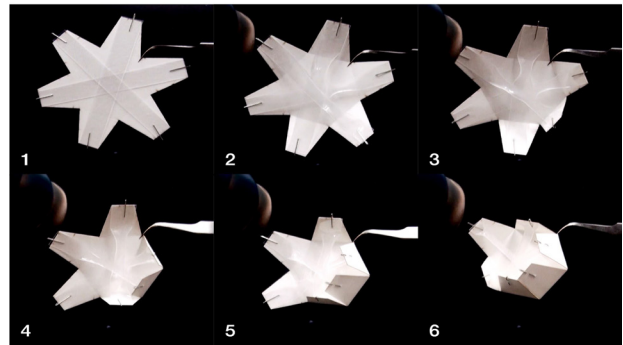


Figure 10. Video stills showing the stages of actuation of the cross-body folding unit made from the SDF-paper system.

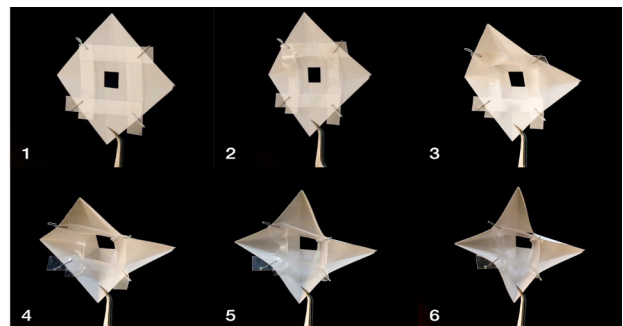
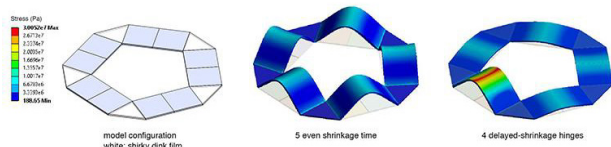


Figure 11. Video stills showing the stages of actuation of the pyramidal unit made from the SDF-paper system.

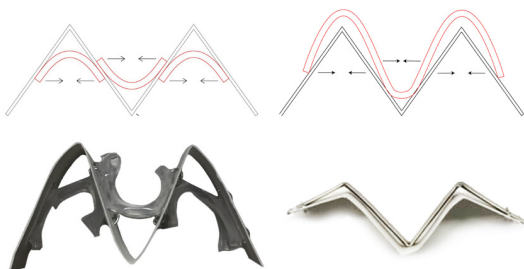
Getting the units to self fold turned out to be a time-related process. While manually folding the inverse-process Enneper surface from the 2D surface, we ran into a problem: every joint has to fold in unison, or it won't fold at all. The issue translated from manual folding, where one can only fold several creases at a time, to self-folding via actuating material.

Placing the actuating material on a joint connected to a larger system of joints — in effect, arranging the joints in series — assumes that every crease in the unit will fold in at once. In the event of non-uniform actuation, the first SDF strips to reach the shrinking temperature threshold has to fight against a stiff body to instigate folding in the unit. If the applied heating is not perfectly uniform, the SDF across the linked creases will actuate at different times. The force of one SDF piece actuating is not enough to allow the joint to fold, and the resulting tension will either tear the joint at the point of stress concentration or tear the SDF strip as it shrinks toward its anchor points, ultimately causing the unit to fail to actuate altogether. (see Figure 12).

Our next iteration attempted to solve this by reinforcing the strength of the actuation by placing the actuating SDF on both sides of the paper joint rather than just one, as had been done for the prior two iterations. (see Figure 13). Applying the logic of this double-sided test piece to a larger unit, we designed the next iteration of the SDF testing unit by combining the cross-body hinge with the valley fold hinge to create a unit with both sets of characteristics. The cross-body folding on this unit allowed the arms to contract from applying heat to the center point, bringing the valley folds together so that they didn't have to fight against a stiff body while the SDF film attached contracted.



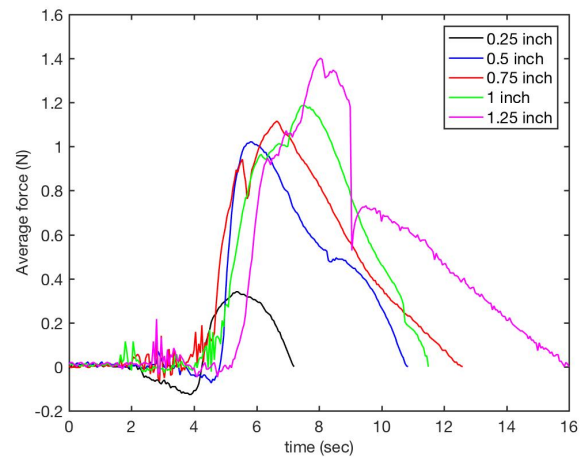
**Figure 12.** Finite element analysis of stress concentration. Left: Shrinking material (white) acting as a folding agent on a kirigami body. Middle: all SDFs actuate at the same time. Right: one SDF actuates earlier than others.



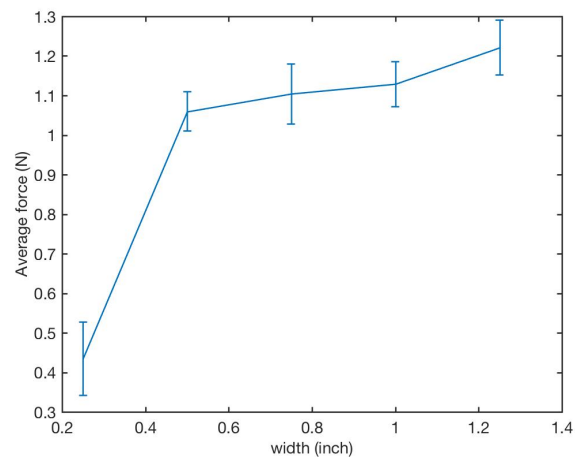
**Figure 13.** Multi-segmented hinge with shrinking material actuating on two sides of sheet material reinforces joint while folding for stronger actuation (Left), Bi-layer hinge by laminating paper with shape memory polymer sheet (Right).

Figure 14 shows that the retracting forces of shrinky dink film with different widths display similar behaviors. The shrinky dink strips actuate at approximately 5 seconds of heat input. The retraction force reaches a maximum peak, then decreases rapidly because the sample strips have reached the polystyrene melting point and fail. Knowing the power of the heat gun, heating time can be translated into energy input by multiplying the time and heat gun power.

The maximum forces of the five different shrinky dink film widths are compared in figure 15. The average force increases as the surface area of the sample increases. The characterization process is repeated ten times for each sample width, and the errors are taken into account.



**Figure 14.** Force curve of shrinky dink films of different widths. Heat is applied at time 0 sec.



**Figure 15.** The maximum force of shrinky dink films of different widths. Error bar is calculated with the standard deviation between the 10 samples of each width.

In contrast to the shrinky dink films, the nitinol wires, which exhibit shape memory alloy behaviors, do not have a failure point. Once the wires reach the maximum force, the force remains constant and is independent of energy input and time.

The last material to be characterized, the SMPs, requires almost equivalent energy input as SMAs (force curve shown in Figure 16). Even though the polymer strips show more noise in actuating, the behavior is still similar to that of the shrinky dink film. The force that the polymers generate reaches a maximum and then decreases as it has reached the threshold temperature. The excessive noise is predicted to be an outcome of the small polymer strip.

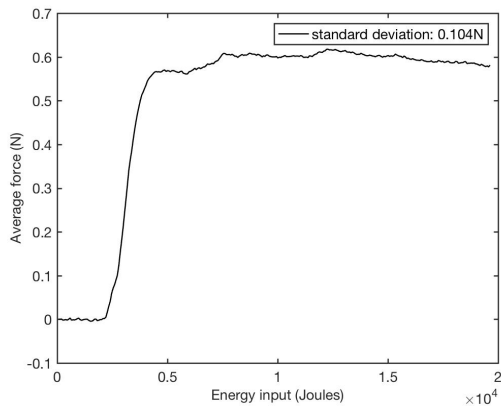


**Figure 16.** Force curve relating to energy input of nitinol wires (SMAs).

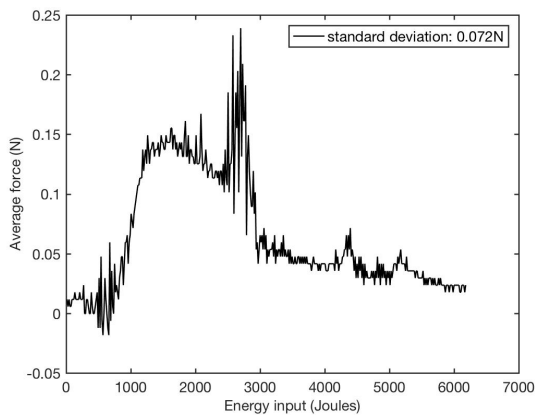


**Figure 17.** Force curve relating to energy input of SMPs.

We compared the results from the SDF experiments with the SMP physical models, finite element analysis simulations, and thermal images (see Figures 18 & 19). We applied the SMP to the hinge part of component model (see Figure 13). The physical models behave as expected after heat actuation, while the thermal images show expected heat concentrations on the models.

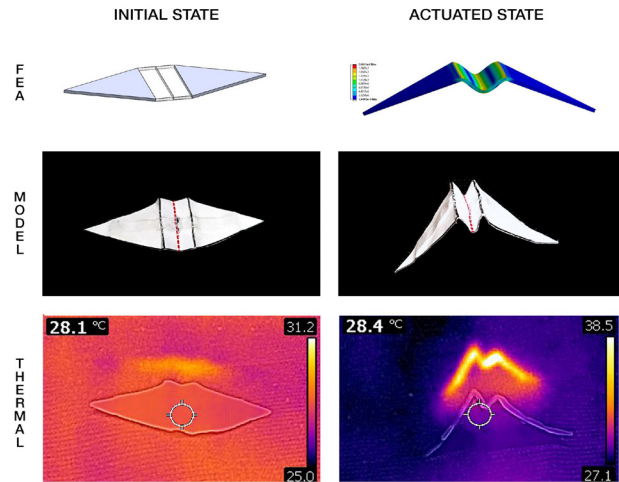


**Figure 18.** Initial state and actuated state of SMPs acting as hinges. A comparison between FEA, physical model, and thermal image.

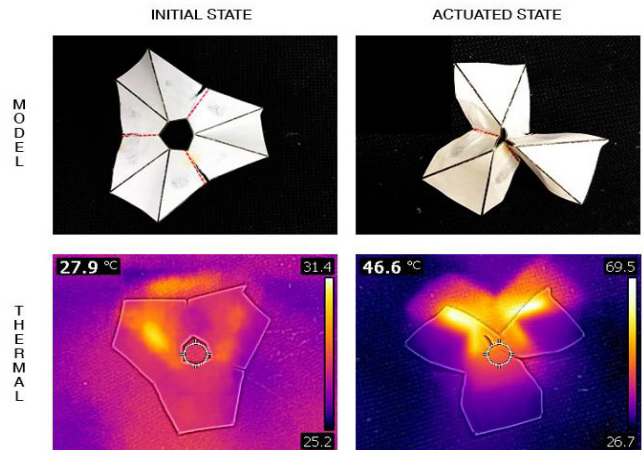


**Figure 19.** Initial state and actuated state of SMPs acting as hinges for a more complex model. A comparison between physical model and thermal image.

#### 4 DISCUSSION

The shrinky dink films characterization results (see Figures 15 & 16) show that the average force the films can generate when actuated by heat increases as the surface area of the sample increases. Figure 15 also shows that the force peaks shifts to the right as width increases. That is, shrinky dink films require more energy input, as well as actuation time, as the surface area increases.

A possible explanation for the noise and the unexpected deviations of force in all material characterization results is due to uneven heating. In the thermal images of Figure 17, temperature density is not even in the geometry. Heat guns emit concentrated heat that is not wide enough to cover all the 3” test samples. This can cause time-related problems described in hinge actuation design. Also, the geometries of both the shrinky dink film and the nitinol wires post actuation may not be completely planar. Changes in Non-planar geometry will lead to complicated forces in 3D space, which

can also lead to the recorded noise and unexpected deviations of force distribution in the characterization results.

Our experiments on hinge actuations demonstrate the possibility of using SDF and SMPs as actuation hinges. While SDF is a single phase irreversible hinge, it is sturdier and has higher stiffness. SMP actuations are reversible, and act as plausible two-way hinges.

Considering that the folding of the hinge is currently passively actuated by the thermal environment by using thermal sensitive material like SMP and SDF, our physical tests are constrained to a small scale. For the next step, we are exploring ways to increase the efficiency of thermal actuation to implement the kirigami folding at the human and architectural scale.

## 5 CONCLUSION

We have established an adequate pipeline for kirigami computational geometry designs, and actuation hinge designs. The flexible, elastic materials we have investigated are shrinky dink films, SMAs, and SMPs. The material properties, both mechanical and thermal, were explored, characterized, and further determined to be adequate to perform as hinge actuation materials. The SDF, SMAs, and SMPs served as the ‘skeletal system’ that actuates the unit. The inactive materials define the kirigami pattern and are the translating body that distributes the actuation forces. Thus, the specificity and design of the kirigami geometry is largely determined by the characterization and distribution of forces.

With physical models serving as proofs of concepts, the pipeline that we established was validated. The kirigami patterns are designed to fold into a 3D surface through simulation. The actuating materials, serving as hinges, provide the forces necessary to reshape the 2D patterns into 3D geometries. The pipeline also serves as a cooperative platform to integrate both designers and engineers. Our next step is to inform kirigami generative design iterations through physical explorations that feature more robust hinge materials. A new dual-material system that combines different actuating materials has the potential to serve as a more robust structural skeletal support with ideal thermal conditions. Now that we have a better understanding of the interactions between different actuating materials (SDF, SMA, & SMP), our current investigations can serve as bases for addressing 2D flat sheet kirigami patterning to 3D form with optimal actuations.

## ACKNOWLEDGMENTS

We thank the Cornell College of Architecture, Art, and Planning for support of this research and the authors gratefully acknowledge the grant from NSF (#NSF 12-583, Award # 1331583).

## REFERENCES

1. Sabin, Jenny E., and Peter Lloyd Jones. *LabStudio: Design Research Between Architecture and Biology*, (London & New York: Routledge Taylor and Francis, 2017).
2. Sabin, Jenny E., et al. “Prototyping Interactive Nonlinear Nano-to-Micro Scaled Material Properties and Effects at the Human Scale” in *Simulation for Architecture and Urban Design (SimAUD)*, April 13-16, 2014.
3. Sabin, Jenny E., et al. “Colorfolds: Eskin+Kirigami, From Cell Contractility to Sensing Materials to Adaptive Foldable Architecture”. *ACADIA 2015*: eds. Lonn Combs and Chris Perry, 2015, 204-209.
4. Eggers, Madeleine, et al. “Matrix Architecture: 3D-Printed and Simulated Kirigami Matrices & Auxetic Materials.” *Symposium on Simulation for Architecture and Urban Design Proceedings 2017*, 2017, pp. 115–121.
5. Huffman, D. A. (1976). Curvature and creases: A primer on paper. *IEEE Transactions on computers*, (10), 1010-1019.
6. Lang, R. J. (1996, May). A computational algorithm for origami design. In *Proceedings of the twelfth annual symposium on Computational geometry* (pp. 98-105). ACM.
7. Felton, S., et al. “A Method for Building Self-Folding Machines.” *Science*, vol. 345, no. 6197, July 2014, pp. 644–646., doi:10.1126/science.1252610.
8. Tachi, T. (2010). Origamizing polyhedral surfaces. *IEEE transactions on visualization and computer graphics*, 16(2), 298-311.
9. Peraire, Jaime, et al. "Adaptive remeshing for compressible flow computations." *Journal of computational physics* 72.2 (1987): 449-466.
10. Piker, Daniel. "Kangaroo: form finding with computational physics." *Architectural Design* 83.2 (2013): 136-137.
11. Behl, Marc, and Andreas Lendlein. “Shape-Memory Polymers and Shape-Changing Polymers.” *Shape-Memory Polymers Advances in Polymer Science*, 2009, pp. 1–40., doi:10.1007/978-3-642-12359-7\_26.